

Spin-Triplet Pairing in Heavy Nuclei is Stable Against Deformation

Georgios Palkanoglou,^{1,2} Michael Stuck,¹ and Alexandros Gezerlis¹

¹*Department of Physics, University of Guelph, Guelph, ON N1G 2W1, Canada*

²*TRIUMF, 4004 Wesbrook Mall, Vancouver, BC V6T 2A3, Canada*

Any experimental evidence of nucleons paired in spin-triplet states will confirm the existence of an exotic phase of nuclear matter. This type of nuclear superfluidity has been hypothesized in heavy nuclei, where the antagonizing spin-orbit effects are damped, and there it oftentimes coexists with traditional spin-singlet pairing, leading to the possibility of mixed-spin pairing. Realistic nuclear deformation, not considered in such studies, could make-or-break these proposals, since its effect on triplet-pairing, and the competition (and coexistence) of the two superfluid phases, was expected to be crucial. We report on a thorough study on the effect of deformation on triplet-, singlet-, and mixed-spin pairing in the relevant region of the nuclear chart. We find that, at low isospin asymmetries, spin-triplet pairing is enhanced by deformation, while below the proton-drip line, the novel superfluid phase survives alongside the usual spin-singlet pairing. These results suggest that spin-triplet superfluidity exists in realistic nuclei and can be probed in the lab.

Introduction Spin-triplet neutron-proton pairs have been elusive, with the only pairing seen in experimentally accessible nuclei being of spin-singlet and between like particles [1]. In contrast, our understanding of nuclear forces tells of an increased attraction in the spin-triplet channel of the two-body nuclear interaction, underlined by the existence of the deuteron. This has generated a long-standing question mark on the existence of deuteron-like spin-triplet pairs in nuclei. At a mean-field level, the strong spin-orbit field has been identified as the suppressor of the spin-triplet superfluidity in nuclei [2, 3], which suggests the possible existence of the exotic superfluid phase in heavy nuclei and extended nuclear systems. At large, nuclear superfluidity remains a vibrant field probed with many approaches [4–12], with ties to astrophysics [13, 15–17] and nuclear reactions [18–21].

Robust spin-triplet pairing has been suggested to exist close to the $N = Z$ line of the nuclear chart, $A \sim 130$, with a region of an exotic mixed-spin condensate lying in the crossover between spin-triplet and spin-singlet pairing [1, 3, 22]. This region of the nuclear chart is characterized by a finite deformation [23], so far neglected in Refs. [3, 22, 24, 25], which could change this picture dramatically: with the two pairing phases in general working against each other, and deformation typically antagonizing pairing altogether [26], the total effect is non-trivial to predict. Furthermore, the existence of spin-triplet pairing in the nuclear ground state relies on the proximity of low- j shells to the Fermi surface that happens in the $A = 130$ region; that too will be altered by deformation. In this Letter, we address nuclear deformation, an important missing piece which can greatly modify pairing correlations: we confirm the existence of spin-triplet pairs in heavy nuclei, at $N = Z$, but also within the physical region, where it coexists with spin-singlet pairing, and can be probed in the lab.

Context We use a generalization of the Hamiltonian used in Refs. [3, 22, 24, 25], which in second quantization reads

$$H = \sum_{ij} \epsilon_{ij} c_i^\dagger c_j + \sum_{i>j,k>l} \langle ij | v | kl \rangle c_i^\dagger c_j^\dagger c_l c_k . \quad (1)$$

The one-body part, ϵ , contains the kinetic energy, a deformed Wood-Saxon well, and a deformed spin-orbit term. At the mean-field level the external Wood-Saxon potential models the shape of the nucleus' surface and the spin-orbit term, peaking at the nuclear surface, is defined on the same shape:

$$\epsilon = \frac{p^2}{2m} + V_{\text{WS}}(\varpi, z; \vec{\alpha}) + C \nabla [V_{\text{WS}}(\varpi, z; \vec{\alpha})] \cdot (\boldsymbol{\sigma} \times \mathbf{p}) . \quad (2)$$

The last term in Eq. (2) is the generalized spin-orbit form that reduces to the familiar $(1/r)dV_{\text{WS}}/dr (\mathbf{1} \cdot \mathbf{s})$ in the absence of deformation [28–30]; it's multiplied by its coupling, C [27]. In lieu of experimental results in the mass region of $A \sim 130$, we follow the predictions of Ref. [23] which prescribe axial deformation for that region with a moderate quadrupole component and small higher-order ones.

The specific shape of the nucleus' surface is given by a vector of deformation parameters, namely, $\vec{\alpha} = (\epsilon, \vec{\beta})$. This contains the elongation of an underlying Cassini oval, ϵ , and the additional deformation described on a basis of spherical harmonics with coefficients β_λ [31, 32]. The vector $\vec{\alpha}$ uniquely defines the nuclear surface,

$$\begin{aligned} \phi(\varpi, z) = & \left[(\bar{z}^2 + \bar{\varpi}^2)^2 - 2\epsilon R_0^2 (\bar{z}^2 - \bar{\varpi}^2) + \epsilon^2 R_0^4 \right]^{1/4} - \\ & - R_0 \left[1 + \sum_{\lambda>0} \beta_\lambda Y_{\lambda 0}(x) \right] = 0 , \end{aligned} \quad (3)$$

and the one-body potential this generates,

$$V_{\text{WS}}(\varpi, z) = V_0 \left[1 + \exp \left(\frac{1}{a} \frac{\phi}{|\nabla \phi|} \right) \right]^{-1} . \quad (4)$$

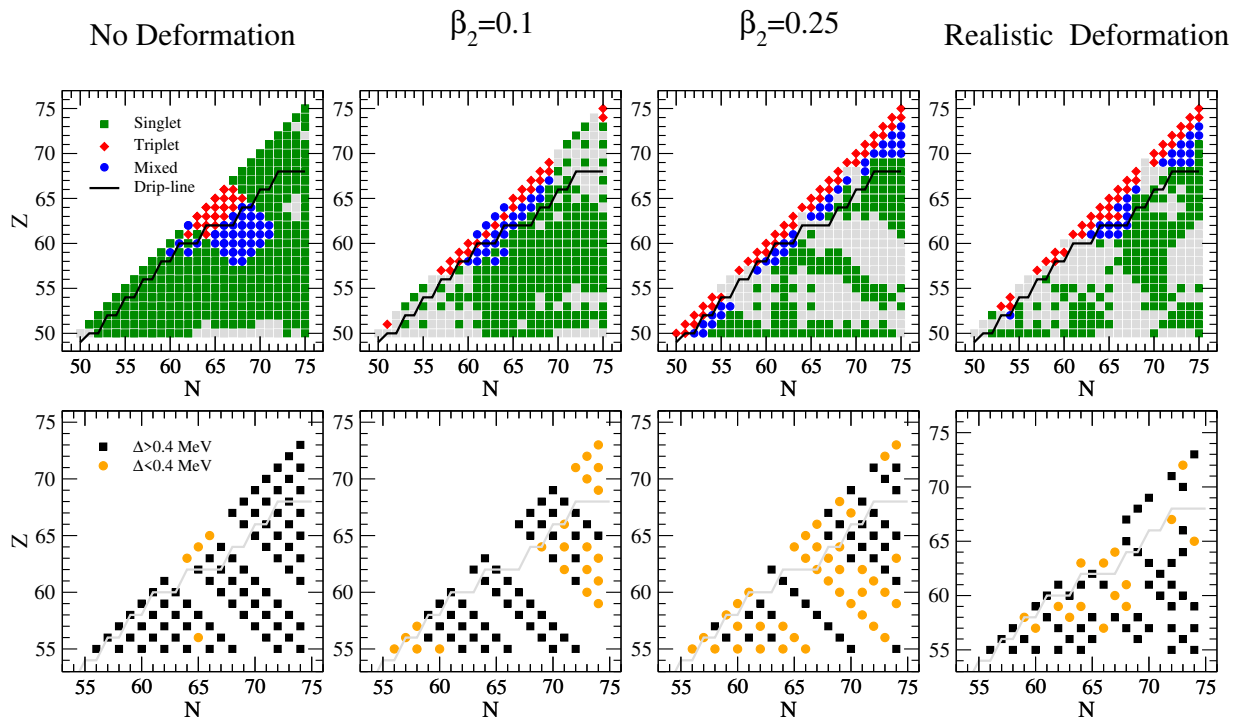


FIG. 1. Chart of nuclides with $Z \leq N$ for neutron numbers from 50 to 75. In the top panels, we show the spin character of the nuclear condensate: the green squares, blue circles, and red diamonds, represent nuclei with singlet, mixed-spin, and triplet pairing, respectively, and the grey squares denote nuclei with $E_{\text{corr}} < 0.5$ MeV. In the bottom panels, we show strong (black squares) and weak (orange circles) pairing gaps (see Eq. (9)) for the same deformation. The proton-drip line is drawn in black in the top panels and in grey in the bottom panels [23].

The barred coordinates, $\bar{\omega} = f(R, x; \varepsilon)$ and $\bar{z} = g(R, x; \varepsilon)$ are cylindrical coordinates parameterized by the curvilinear coordinates (R, x) in which Cassini ovals span coordinate surfaces and R_0 and a are the radius and surface diffuseness, respectively, of the undeformed nucleus.

The two-body part of the Hamiltonian, v , is a contact pairing interaction,

$$\langle ij | v | kl \rangle = \sum_{\alpha} v_{\alpha} \langle ij | \delta^{(3)}(\mathbf{x} - \mathbf{x}') P_{\alpha} P_{J_z=0} | kl \rangle, \quad (5)$$

where the projection operator P_{α} projects on six spin-isospin channels: $\alpha = 0, 1, 2$ correspond to the three spin-singlet and isospin-triplet channels, while $\alpha = 3, 4, 5$ correspond to the three spin-triplet and isospin-singlet channels. The projection operator $P_{J_z=0}$ takes advantage of the axial symmetry and pairs particles in time reversed states, resulting in axially-symmetric pair-wavefunctions. It conveniently generalizes the common approximation of pairs with zero orbital angular momentum[1, 3] allowing formation of pairs with finite angular momentum which are expected to form in ground-states of deformed nuclei. Similar pairing schemes have been used before in the study of spin-singlet and spin-triplet nuclear pairing [33, 34]. The interaction strengths that appear in Eq. (5) are the same as in earlier works [3, 22, 24, 25].

We allow for six pairing channels, the three spin-singlet and three spin-triplet ones defined in Eq. (5). Channels with the same total spin (or isospin) and different projections are prescribed the same v_{α} and are seen as equivalent, that is, we use an interaction with only two interaction strengths.

HFB treatment and its application The Hartree-Fock-Bogolyubov (HFB) treatment of the Hamiltonian in Eq. (1) corresponds to identifying the Bogolyubov transformation that minimizes the ground-state energy. The system is then described as a collection of free quasiparticles, whose vacuum defines the ground-state. In practice, the Bogolyubov transformation is parameterized by the matrices U and V , which mix particle and hole operators in Fock-space defining the quasi-particles. These matrices also define the normal and anomalous densities, $\rho = V^* V^T$ and $\kappa = V^* U^T$, respectively, which are fundamental to the description, as they in turn define the HFB expectation value of the Hamiltonian,

$$H^{00} = \text{Tr} \left[\epsilon \rho - \frac{1}{2} \Delta \kappa^* \right], \quad (6)$$

where $\Delta_{ij} = \frac{1}{2} \sum_{kl} v_{ijkl} \kappa_{kl}$.

The HFB treatment can be implemented very effectively via the gradient method outlined in Ref. [35], and

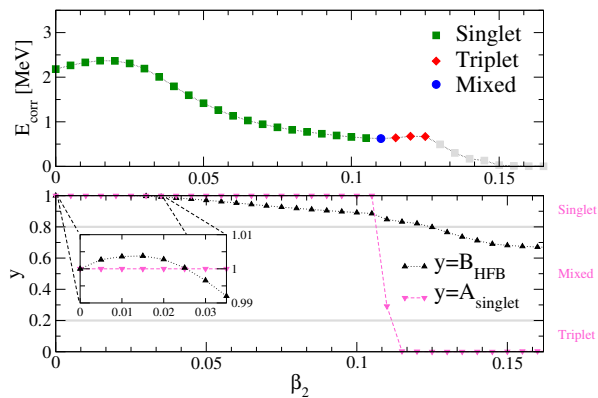


FIG. 2. The evolution of $^{108}_{54}\text{Xe}$'s ground state increasing quadrupole deformation. The top panel shows the correlation energy of the nucleus. In the lower panel, A_{singlet} measures the size of the singlet condensate, relative to the triplet condensate (see Eq. (7)) and B_{HFB} quantifies the spin-orbit field (see Eq.(8)).

used in a similar fashion as in Refs. [3, 22, 24]: we locate the HFB minimum by performing a gradient descent on the surface of the HFB energy parametrized by the U and V matrices (or κ) in Eq. (6). In this way one can straightforwardly identify solutions of different symmetries by constraining the descent, i.e., introducing the appropriate terms with Lagrange multipliers to Eq. (6). We use 8 constraining fields: the neutron and proton numbers and six pairing amplitudes which are defined below. This allows us to explore different HFB minima, apart from the global minimum that corresponds to the fully-paired ground state.

The spin character of an HFB state can be described by the expectation value of the pair operator $\bar{P}_\alpha = P_\alpha P_{J_z=0}$ that defines the six pairing channels and appears in Eq. (5). These six pairing amplitudes can then be used as constraining fields to locate states with certain pairing character. Specifically, we use the state where all six pairing channels are closed, i.e., all pairing amplitudes vanish, as a reference state: we measure all energies relative to its unpaired energy, namely, E_0 , and call the resulting quantity correlation energy, $E_{\text{corr}} = E - E_0$.

Results We mainly characterize our results by the strength and spin character of their pairing. We quantify the strength of the pairing correlations via the correlation energy. We label the spin character of the condensate using the expectation values of the pairing fields $K_\alpha = \langle \bar{P}_\alpha \rangle$. We define [22]:

$$A_{\text{singlet}} = \frac{\sum_{\beta=0,1,2} K_\beta^2}{\sum_\alpha K_\alpha^2}, \quad (7)$$

and a nucleus is labeled as spin-singlet if $A_{\text{singlet}} > 0.8$ and spin-triplet if $A_{\text{singlet}} < 0.2$, otherwise, the nucleus is labeled as mixed-spin. Finally, the spin-orbit field is

expected to play a major role in the interplay of the different pairing phases, and we quantify it via its expectation value at the HFB ground state:

$$B_{\text{HFB}} = \langle \text{HFB} | C \nabla f(\rho, z; \vec{\alpha}) \cdot (\boldsymbol{\sigma} \times \mathbf{p}) | \text{HFB} \rangle. \quad (8)$$

We calculate correlation energies and pairing amplitudes for all nuclei in the interesting region of mass $A \sim 130$ and we plot the results in the top panels of Fig. 1. To visualize how the condensates respond to nuclear deformation, we perform these calculations for a sequence of deformation parameters, starting from spherical shapes across the region in the leftmost panel, which reproduces the results of Refs. [3, 22], increasing quadrupole deformation for all nuclei progressively in the two middle panels, and reaching the realistic deformation prescribed by Möller *et al* [23] in the rightmost panel. The bottom panels of Fig. 1 show pairing gaps, i.e., binding energies of pairs, for the region of interest and for the same deformation parameters. These will be discussed later.

The superfluidity's response to deformation is rich so we start from the $N = Z$ line, where neutrons and protons occupy the same orbitals, increasing the odds for neutron-proton pairing. First, we investigate quadrupole deformation (β_2), which seems to drive the qualitative effects for most nuclei. At very small β_2 deformation, spin-triplet pairing is generally damped, resulting in a small increase in the correlation energies of singlet nuclei and the change of some triplet paired nuclei to mixed-spin. This can be seen at $A \sim 125$ in Fig. 1 as well as the low-deformation end of Fig. 2. As quadrupole deformation approaches the realistic value predicted by Ref. [23] for the region, spin-triplet completely dominates the $N = Z$ line inducing a mixed-spin band at $N - Z = 2$ or 3 before the nuclear condensate turns spin-singlet. This dramatic change resembles the results of Ref. [24], where the spin-orbit interaction was switched-off artificially: the enhancement of spin-triplet pairing can be understood as driven by a general suppression of the spin-orbit field at the ground-state. This is clearly demonstrated in Fig. 3 for $^{126}_{61}\text{Pm}$ where the spin-singlet component and the spin-orbit field show similar behavior. The connection can also be seen in Fig. 2 where we plot the correlation energy, spin-singlet pairing amplitude, and spin-orbit field for $^{108}_{54}\text{Xe}$, a case of a pure spin-singlet paired ground state at the spherical limit turned to spin triplet by deformation. There the transition between the two pairing-phases is accompanied by a steady decrease of the spin-orbit field.

On the $N = Z$ line, a reduced spin-orbit field corresponds to a spin-triplet paired ground-state [3, 24]. Moving along an isobar (i.e., increasing $N - Z$) the nuclear condensate very quickly changes to spin-singlet. This is expected, as increasing isospin asymmetry translates to increasing mismatch in the proton and neutron Fermi

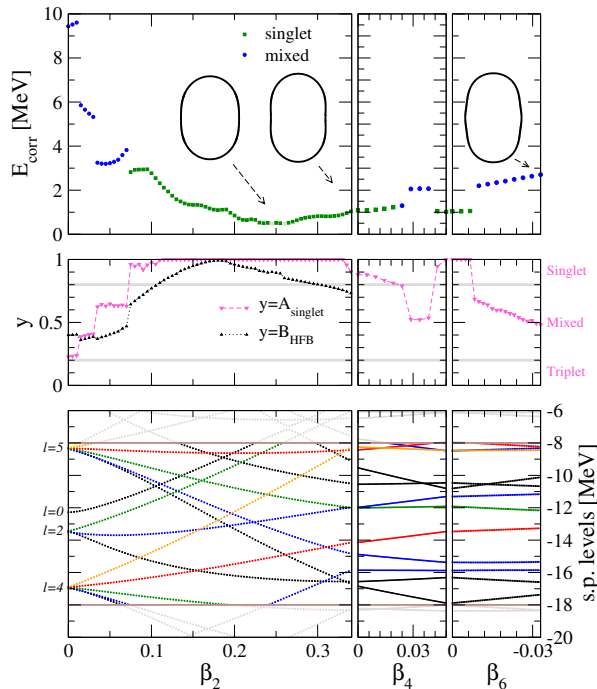


FIG. 3. The evolution of $^{126}_{61}\text{Pm}$'s ground state from no deformation to the realistic deformation predicted by Ref. [23]. The bottom panel shows the evolution of the single-particle levels that lie in the energy window: from bottom to top $l_z = 0$ (black), 1 (blue), 2 (green), 3 (red), 4 (orange), and 5 (yellow). The middle panel shows the singlet pairing amplitude overlaid with the expectation value of the spin-orbit field (at the ground-state), appropriately normalized. The top panel shows the correlation energy of the nucleus along with the shape of the nuclear surface along the evolution.

surfaces, making the pairing of a neutron and a proton increasingly unlikely.

Switching-on the higher deformation modes, to the values predicted by Ref. [23], we find that for most nuclei, qualitatively, the picture doesn't change: spin-triplet pairing dominates at and around $N = Z$, mixed-spin nuclei can be found at small isospin asymmetry $N - Z$, and spin-singlet generally takes over for higher isospin asymmetries. Additionally, the cross-over region, between the two phases has been drastically reduced compared to the spherical limit. At a triangular region, close to $N = Z$, at $A \sim 130$ some triplet- and mixed-spin paired nuclei re-emerge, driven by higher-order deformation, with some isotopes of Pm ($Z = 61$) also being inside the physical region. Specifically, the nuclei $^{125}_{61}\text{Pm}$, $^{126}_{61}\text{Pm}$, and $^{127}_{61}\text{Pm}$ pose an interesting case as they lie within the proton drip-line and maintain a sizeable spin-triplet condensate at full deformation. These nuclei also exhibit a comparable spin-singlet condensate, co-existing with the spin-triplet, making them of mixed-spin character.

In the survey of the region presented in Fig. 1 we iden-

tify some Pm isotopes that lie in the physical region, i.e., within the proton drip-line and can support spin-triplet pairing in their ground states. With all three nuclei parameterized with similar realistic deformation parameters, we plot the evolution of $^{126}_{61}\text{Pm}$ in Fig. 3 where it is seen that it's the higher-order deformation that drives this transition. Plotted in the same figure is also the evolution of the single-particle levels (bottom panel) demonstrating how the overall initial reduction in the correlation energy is driven by the reduction of the single-particle degeneracy close to the Fermi surface; the latter lies close to the middle of the indicated energy window. Finally, overlaid on the top panel, are the shapes of the nuclear surfaces at various deformations demonstrating a simple connection between correlation energy (or pairing) and the geometry of the nucleus.

The source of the spin-orbit field's decrease needs a deeper discussion. We find that the matrix elements of the spin-orbit generally decrease within each j_z -shell with increasing quadrupole deformation. Even when some elements increase, the determinant of the average j_z -shell block decreases, signaling a decrease of the spin-orbit field's eigenvalues. This suppression is especially counter-intuitive since the spin-orbit field is a surface effect and deformation is moving the nuclear surface away from the spherical shape, which has the lowest surface-to-volume ratio, for a given volume. Indeed, perturbative calculations, for very small quadrupole deformation, show that an increase in the spin-orbit strength is expected, if the nuclear surface is adequately probed by the participating orbitals. A typical example of such an increase is seen in the low- β_2 region of Fig. 2. Hence, the existence and/or extent of a spin-orbit increase, depends on whether deformation brings higher- j orbitals close to the nucleus' Fermi surface. This is because high- j wavefunctions lie closer to the nuclear surface and as such can more efficiently probe surface effects. A very pronounced increase can be seen in $^{126}_{61}\text{Pm}$, at low β_2 deformation, where $l = 5$ and $l = 4$ states are brought closer to the Fermi surface (i.e., the chemical potential). This increase in the spin-orbit field's strength suppresses spin-triplet pairing allowing the correlation energy of spin-singlet nuclei to increase. However, the strength of the spin-orbit field is then quickly suppressed when increasing deformation drives the $l = 4, 5$ orbitals away from the Fermi surface. It's important to clarify that this suppression is *not* an effect of pairing, as it is seen both in the HFB state and the unpaired state, and it is traced back to the reduction of the spin-orbit's matrix elements, mentioned above. The above suggest a general suppression of the spin-orbit mean field by nuclear deformation.

Outlook This Letter constitutes the first systematic study of the interplay between spin-singlet pairing, spin-triplet pairing, and deformation in nuclei and it demonstrates that the deformation's effect on superfluidity can be understood as ternary. Firstly, it weakens all types of

pairing correlations by reducing the single-particle density of states, as has been shown in the past. Secondly, it increases the surface-to-volume ratio of a given nucleus amplifying the spin-orbit field's effect, which in turn tends to suppress spin-triplet pairing. Finally, by changing the single-particle level structure close to the Fermi surface, it might induce pairing of particles in low- j orbitals, whose wavefunctions don't lie very close to the nucleus' surface, thus lifting the spin-orbit field's suppression and enhancing spin-triplet pairing. The interplay of the three effects, coupled with the well-documented antagonism of the two superfluid phases, gives rise to an unexpected outcome in the mass region of $A \sim 130$: realistic deformation creates a spin-triplet superfluid in the ground states of most nuclei with $N = Z$, and on some nuclei with small isospin asymmetry where it almost always coexists with a spin-singlet superfluid phase. The spin triplet phase, be it pure or mixed, was found to be moderately strong, yielding correlation energies of ~ 2 MeV for realistically deformed nuclei.

The correlation energies are a valuable tool in visualizing pairing correlations since they can be seen as the binding energy that a nucleus gains from the pairing correlations. However, they are *not* experimentally observable. Therefore, we also calculated pairing gaps, via the familiar odd-even staggering, traditionally the smoking gun of superfluidity in nuclear systems [1, 37],

$$\Delta(N) = E(N) - \frac{1}{2} [E(N-1) + E(N+1)] , \quad (9)$$

where N is either a proton or a neutron, and an odd number, while the other nuclear species is kept to a fixed even number [38]. We plot the results in the bottom panel of Fig. 1. We distinguish between gaps larger and smaller than 0.4 MeV, while we have excluded results with systematic errors generated by the existence of an energy window (i.e., a hard cut-off) in the single-particle spectrum (see Fig.3). That way, the rightmost panel of the lower row in Fig. 1 adds nuance to the conventional wisdom dictating that deformation generally suppresses pairing. That is, deformation of higher multipoles tends to strengthen pairing correlations, compared to pure quadrupole deformation, seen both in the pairing gaps of Fig. 1 and the correlation energies of Fig. 3. Finally, Refs. [3, 22], demonstrated that spin-triplet paired ground states yielded reduced pairing gaps, but Fig. 1 shows that deformation partially lifts this suppression. This was accurately predicted in Ref. [1] and an inspection of the pairing gaps adds detail: as quadrupole deformation increases, the drop in the pairing gaps at $A \sim 130$ rises while the rest of the gaps on the $N = Z$ line steadily decrease, resulting in an even distribution of pairing gaps along the $N = Z$ line. A similar effect is seen in the correlation energies as well, where increasing quadrupole deformation equalizes the relatively large correlation energies of the non-deformed triplet-paired nuclei, resulting

in a less variable distribution of correlation energies at realistic β_2 deformation. These effects can be attributed to the fragmentation of the l -shells that is induced by deformation and demonstrated in the lowest panel of Fig. 3.

In general we identify an enhancement of spin-triplet pairing in the ground-states of realistically deformed nuclei with $N \sim Z$ and $A \sim 130$. While indirect evidence of this enhancement is available in the literature [26, 39, 40], the complete take-over, or the connection with the spin-orbit field's suppression by the scarcely sampled nuclear surface is new here. The latter suppression is encountered circumstantially in calculations of hypernuclei [41] where the spin-orbit strength is routinely quenched to achieve the right quadrupole deformation, and in the investigations of Ref. [42], where increasing the spin-orbit coupling makes the mean-field ground-state of light nuclei take spherical shape. Similar conclusions were drawn in Ref. [36] where deformation seems to antagonize the energy splitting induced by spin-orbit in some heavy nuclei in the region of $A \sim 160$. Consistently with our arguments, all these nuclei have several low- j orbitals close to their Fermi surfaces.

Our results predict the existence of spin-triplet pairs in heavy nuclei and invite further accurate yet costly *ab initio* calculations [12, 43]. Additionally, the existence of exotic pairing phases in heavy deformed nuclei may lead to other interesting phenomena, e.g., in nuclear dynamics, fission and fusion [19, 20, 44, 45], or nuclear structure [46–48] and reactions [21]. Finally, our results can be significant for experiments as we have identified some nuclei on or below the proton drip-line, which can be accessed by experiment most easily, with a sizeable spin-triplet condensate when deformed. These nuclei have a mixed-spin pairing character since they exhibit a comparable co-existing singlet condensate. Various signatures of spin-triplet pairing in the nuclear ground state have been proposed: an enhanced cross-section for np transfer [1, 49], the sign of neutron-proton spin-spin correlations [50] (but also see Ref. [51]), or similarities between spectra of odd-odd and even-even nuclei [52]. The rest of the spin-triplet condensates lie beyond the proton drip-line where they could be probed in resonance states, though such experiments are more demanding because of the short lifetimes of these states. Hence, these results hold the promise of finding this sought-after nuclear pairing in the lab and additionally elucidating the physics of mixed-spin paired nuclei.

We thank P. Garrett, T. Papenbrock, P. Navratil, M. Drissi, L. Jokiniemi, E. Leistenschneider, and A. Kwiatkowski for useful discussions. This work was supported by the Natural Sciences and Engineering Research Council (NSERC) of Canada and the Canada Foundation for Innovation (CFI). TRIUMF receives federal funding via a contribution agreement with the National Research Council of Canada. Computational resources were provided by SHARCNET and NERSC.

-
- [1] S. Frauendorf and A. O. Macchiavelli, *Prog. Part. Nucl. Phys.* **78**, 24 (2014).
- [2] A. Poves and G. Martinez-Pinedo, *Phys. Lett. B* **430**, 203 (1998).
- [3] G. F. Bertsch and Y. Luo, *Phys. Rev. C* **81**, 064320 (2011).
- [4] V. Somà, T. Duguet, and C. Barbieri, *Phys. Rev. C* **84**, 064317 (2011).
- [5] S. Gandolfi, G. Palkanoglou, J. Carlson, A. Gezerlis, K. E. Schmidt, *Condens. Matter* **2022** **7**, 19 (2022).
- [6] C. Barbieri, T. Duguet, and V. Somà, *Phys. Rev. C* **105**, 044330 (2022).
- [7] M. Drissi, A. Rios, and C. Barbieri, arXiv:2107.09759.
- [8] P. Schuck and M. Urban, *Phys. Rev. C* **100**, 031301 (2019).
- [9] A. Pérez-Obiol, S. Masot-Llima, A. M. Romero, J. Menéndez, A. Rios, A. García-Sáez, and B. Juliá-Díaz, *Eur. Phys. J. A* **59**, 240 (2023).
- [10] N. Hinohara and W. Nazarewicz, *Phys. Rev. Lett.* **116**, 152502 (2016).
- [11] N. Hinohara, T. Oishi, K. Yoshida, arXiv:2308.02617.
- [12] A. Tichai, P. Arthuis, T. Duguet, H. Hergert, V. Somà, and R. Roth, *Phys. Lett. B* **786**, 195 (2018).
- [13] A. Sedrakian and J. W. Clark, *Eur. Phys. J. A* **55**, 167 (2019).
- [14] A. Pastore, *Phys. Rev. C* **91**, 015809 (2014).
- [15] N. Martin and M. Urban, *Phys. Rev. C* **94**, 065801 (2016).
- [16] A. Sourie and N. Chamel, *MNRAS* **503**, 1407 (2021).
- [17] A. Rios, A. Polls, and W. H. Dickhoff, *J. Low Temp. Phys.* **189**, 234 (2017).
- [18] T. Oishi, M. Kortelainen, and A. Pastore *Phys. Rev. C* **96**, 044327 (2017).
- [19] P. Magierski, K. Sekizawa, and G. Wlazlowski, *Phys. Rev. Lett.* **119**, 042501 (2017).
- [20] R. Bernard, S. A. Giuliani, and L. M. Robledo *Phys. Rev. C* **99**, 064301 (2019).
- [21] Y. F. Niu, Z. M. Niu, G. Colò, and E. Vigezzi, *Phys. Lett. B* **780**, 325 (2018).
- [22] A. Gezerlis, G. F. Bertsch, and Y. L. Luo, *Phys. Rev. Lett.* **106**, 252502 (2011).
- [23] P. Möller, A. Sierk, T. Ichikawa, H. Sagawa, *At. Data Nucl. Data Tables* **109**, 1 (2016).
- [24] B. Bulthuis and A. Gezerlis, *Phys. Rev. C* **93**, 014312 (2016).
- [25] E. Rrapaj, A. O. Macchiavelli, and A. Gezerlis, *Phys. Rev. C* **99**, 014321 (2019).
- [26] D. Gambacurta and D. Lacroix, *Phys. Rev. C* **91**, 01430 (2015).
- [27] A. Bohr and B. Mottelson, *Nuclear Structure*, Vol. I (Benjamin, New York, 1969).
- [28] M. Bender, P.-H. Heenen, and P.-G. Reinhard, *Rev. Mod. Phys.* **75**, 121 (2003).
- [29] E. Terán, V. E. Oberacker, and A. S. Umar, *Acta Physica Hungarica A* **16**, 437–446 (2002).
- [30] E. Terán, V. E. Oberacker, and A. S. Umar *Phys. Rev. C* **67**, 064314 (2003).
- [31] V. S. Stavinsky, N. S. Rabotnov and A. A. Seregin, *Yad. Fiz.* **7**, 1051 (1968).
- [32] V. V. Pashkevich, *Nucl. Phys. A* **169**, 2 (1971).
- [33] N. Sandulescu, D. Negrea, and D. Gambacurta, *Phys. Lett. B* **751**, 348 (2015).
- [34] D. Negrea, P. Baganu, D. Gambacurta, and N. Sandulescu *Phys. Rev. C* **98**, 064319 (2018).
- [35] L. M. Robledo and G. F. Bertsch, *Phys. Rev. C* **84**, 054302 (2011).
- [36] K. Takahasi, *J. Phys. Soc. Jpn.* **17**, 1229 (1962).
- [37] G. Palkanoglou, F. K. Diakonov, and A. Gezerlis, *Phys. Rev. C* **102**, 064324 (2020).
- [38] T. Duguet, P. Bonche, P.-H. Heenen, and J. Meyer, *Phys. Rev. C* **65**, 014311 (2001).
- [39] J. Terasaki, R. Wyss, and P.-H. Heenen, *Phys. Lett. B* **437**, 1 (1998).
- [40] D. Negrea, N. Sandulescu, and D. Gambacurta, *Phys. Rev. C* **105**, 034325 (2022).
- [41] H.-J. Schulze, M. T. Win, K. Hagino, and H. Sagawa, *Prog. Theor. Phys.* **123**, 569 (2010).
- [42] G. Ripka, *Adv. Nucl. Phys.* **1**, 183 (1968).
- [43] H. Hergert, S. K. Bogner, S. Binder, A. Calci, J. Langhammer, R. Roth, and A. Schwenk, *Phys. Rev. C* **87**, 034307 (2013).
- [44] G. Scamps, D. Lacroix, G. F. Bertsch, and K. Washiyama, *Phys. Rev. C* **85**, 034328 (2012).
- [45] J. Sadhukhan, J. Dobaczewski, W. Nazarewicz, J. A. Sheikh, and A. Baran, *Phys. Rev. C* **90**, 061304(R) (2014).
- [46] V. V. Baran, D. R. Nichita, D. Negrea, D. S. Delion, N. Sandulescu, and P. Schuck, *Phys. Rev. C* **102**, 061301(R).
- [47] M. Sambataro and N. Sandulescu, *Phys. Lett. B* **(820)**, 136476 (2021).
- [48] M. Sambataro, N. Sandulescu, and D. Gambacurta, *Nucl. Phys. A* **1036**, 122675 (2023).
- [49] H. Sagawa, C. L. Bai, and G. Colò, *Phys. Scr.* **91**, 083011 (2016).
- [50] H. Matsubara et al., *Phys. Rev. Lett.* **115**, 102501 (2015).
- [51] P. Van Isacker and A. O. Machiavelli, *Eur. Phys. J. A* **57**, 178 (2021).
- [52] S. Frauendorf, *Rev. Mod. Phys.* **73**, 463 (2001).